RHEA v1.0: Enabling fully coupled simulations with hydro-geomechanical heterogeneity

Jose M. Bastias Espejo[1], Andy Wilkins[2], Gabriel C. Rau[1,3], and Philipp Blum[1]

[1]Karlsruhe Institute of Technology, Institute of Applied Geosciences, Karlsruhe, Germany
[2]Commonwealth Scientific and Industrial Research Organisation (CSIRO), Mining Geomechanics Team, Brisbane, Australia
[3]The University of New South Wales, Connected Waters Initiative Research Centre, Sydney, Australia

Correspondence: Jose Bastias (jose.bastias@kit.edu)

Abstract. Realistic modelling of tightly coupled hydro-geomechanical processes is relevant for the assessment of many hydrological and geotechnical applications. Such processes occur in geologic formations and are influenced by natural heterogeneity. Current numerical libraries offer capabilities and physics couplings that have proven to be valuable in many geotechnical fields like gas storage, rock fracturing and Earth resources extraction. However, implementation and verification of full heterogeneity of subsurface properties using high resolution field data in coupled simulations has not been done before. We develop, verify and document RHEA (Real HEterogeneity App), an open-source, fully coupled, finite-element application capable of including element-resolution hydro-geomechanical properties in coupled simulations. We propose a simple, yet powerful workflow to allow the incorporation of fully distributed hydro-geomechanical properties. We then verify the code with analytical solutions in one and two dimensions, and propose a benchmark semi-analytical problem to verify heterogeneous systems with sharp gradients. Finally, we demonstrate RHEA's capabilities with a comprehensive example including realistic properties. With this we demonstrate that RHEA is a verified open-source application able to include complex geology to perform scalable, fully coupled, hydro-geomechanical simulations. Our work is a valuable tool to assess challenging real world hydro-geomechanical systems that may include different levels of complexity like heterogeneous geology with several time and spatial scales and sharp gradients produced by contrasting subsurface properties.

1 Introduction

The complexity of processes occurring in fluid saturated deformable porous media and their importance to a wide range of subsurface applications presents a major challenge for numerical modelling especially when including realistic heterogeneity. Example applications in geo-engineering that inherently require coupling of hydro-geomechanical processes are the interaction between pressure, flow and fracturing of rocks (Atkinson, 2015; Weng, 2015; Berre et al., 2019), land surface subsidence caused by the extraction of Earth resources (Peng, 2020; Ye et al., 2016), underground gas storage (Yang et al., 2016; Tarkowski, 2019) and mass movement (Zaruba and Mencl, 2014; Haque et al., 2016; Gariano and Guzzetti, 2016). Even though the fundamental mathematical description of coupled hydro-geomechanical processes has reached general consensus (Cheng, 2016; Wang, 2017), realistic modelling of such processes requires a precise description of the underground.

Heterogeneity is ubiquitous across scales and strongly affects the mechanical properties as well as the movement of fluids

25 through the subsurface. For instance, the hydraulic conductivity of fractures within a porous rock is often orders of magnitude greater than that of unfractured rock, so that fine spatial discretization around fractures is needed in certain numerical models, resulting in infeasible computational demands (Morris et al., 2006; Eaton, 2006). As a result, the development of coupled hydro-geomechanical models generally requires simplifying or averaging heterogeneity, i.e. homogenising (Blum et al., 2005, 2009). Recent research has identified the need to improve modelling of coupled hydro-geomechanical systems (Lecampion

30 et al., 2018; Grigoli et al., 2017; Birkholzer et al., 2019), and particularly also the importance of introducing high-resolution details to improve the accuracy of numerical simulations (McMillan et al., 2019).

Terzaghi (1923) first described the elastic interactions between a porous media and a fluid occupying its pore space, and the unidirectional system's dynamic responses to external forces. Biot (1941) later generalised this theory to three dimensions giving rise to the well-known theory of consolidation or poroelasticity, also termed *Biot* theory. Since the 1970's, a large

35 number of numerical libraries have been developed, optimised and applied to a diverse range of poroelastic applications (Bear and Verruijt, 1987; Verruijt, 1995; Cundall and Hart, 1993; Boone and Ingraffea, 1990). Notable is the work of Verruijt (2013), who designed a number of numerical solvers for typical one and two dimensional poroelastic problems.

Current subsurface hydro-geomechanical simulation codes can be classified based on the numerical solution scheme and modelling approach of the coupled physics. For example, sequential coupling solves for the hydraulic and geomechanical

40 variables independently and in sequence. Notable examples are geomechanics models based on TOUGH (Transport Of Unsaturated Groundwater and Heat) (Pruess et al., 1999; Xu et al., 2006; Lei et al., 2015; Lee et al., 2019). These consist of different libraries to solve for coupled thermo-hydro-mechanical (THM) applications relying on the numerical capabilities provided by TOUGH. The libraries differ in their fundamental equations, numerical solution methods and discretization schemes (Rutqvist, 2017). Although sequential codes allow flexible and efficient code management in conjunction with reasonable computational

45 costs, they tend to perform poorly in tightly coupled processes, since transient interaction between variables may not be computed accurately (Kim et al., 2011; Beck et al., 2020).

Another concept is to solve the hydro-geomechanical equations as a fully-coupled system (i.e. all equations are solved simultaneously). This is often performed using an implicit time-stepping scheme, which has unconditional numerical stability and high accuracy, but is computationally expensive. This approach has proven to be useful in geo-engineering applications

50 (Nghiem et al., 2004; Hein et al., 2016; Pandey et al., 2018). Various fully coupled hydro-geomechanical libraries have been developed and released. Proprietary software such as COMSOL (Holzbecher, 2013) has been used intensively in geomechanical applications, in particular for modelling of coastal aquifers (Zhao et al., 2017). More recently, Pham et al. (2019) included geomechanical and poroelastic capabilities into the proprietary groundwater modelling environment FEFLOW (Finite Element Flow). Notably also, two open source Python codes have been developed. The first is the FEniCS project (Haagenson et al.,

55 2020; Alnæs et al., 2015), while the second is called Porepy and was specifically developed to simulate THM processes in rock fractures (Keilegavlen et al., 2017). Despite the fact that python-based coding offers the advantage of high-level programming within a relatively friendly user interface, these codes are in an immature stage and relevant subsurface boundary conditions such as point and line sinks have not yet been integrated.

An additional option is OpenGeoSys, a well-known open source library to solve multi-phase and fully coupled THM physics
60 (Kolditz et al., 2012). While the code is well documented and features several examples in different subsurface areas, its
fundamental governing equations are fixed and it lacks a flexible API to customise them. Furthermore, the authors are unaware
of a peer-reviewed verification which includes full geomechanical heterogeneity.

The multi-physics coupling framework MOOSE (Multiphysics Object Oriented Simulation Environment) (Permann et al.,
2020) offers a unique environment where users can couple different physical processes in a modular approach. Within the
65 object-oriented ecosystem of MOOSE, each physical process (or its partial differential equation, PDE) is treated separately as
an individual object and coupling is automatically performed. The MOOSE numerical scheme is based on the finite element
(FE) method. It offers gold-standard numerical solvers as well as a host of useful features such as adaptive meshing. MOOSE
enables the user to focus on describing the governing equations while the underlying numerical technicalities are taken care
of by the system. We have found that mastering the basic concepts of the MOOSE workflow requires a steep learning curve.
70 However, the benefits are significant, for example an experienced user can easily modify the source code to add desired features
such as multi-scale physics, non-linear material properties, complex boundary conditions or even basic post-processing tools.

An example of MOOSE's capabilities in simulating coupled processes in porous media was illustrated by Cacace and
Jacquey (2017), who developed a MOOSE-based application named GOLEM. It was optimised to model three-dimensional
THM processes in fractured rock (Freymark et al., 2019). However, a more robust implementation is Porous Flow, an embedded
75 MOOSE library to simulate multi-phase flow and THMC processes in porous media (Wilkins et al., 2020). Porous Flow has
been verified and applied to simulate a number of complex and realistic systems, for example shallow geothermal systems
(Birdsell and Saar, 2020), CO_2 sequestration (Green et al., 2018) and groundwater modelling with plastic deformation (Herron
et al., 2018). However, it has not yet been extended and verified for the simulation of spatial heterogeneity.

The aim of this paper is therefore to develop, verify and illustrate a novel and generic workflow for modelling fully cou-
80 pled hydro-geomechanical problems allowing the inclusion of hydraulic and geomechanical heterogeneity inherent to realistic
geological systems. We call this workflow RHEA (Real HEterogeneity Application). This name is motivated by the MOOSE
tradition of using animal names: Rhea is a flightless bird that is native to the South American continent. RHEA is based on
MOOSE's modular ecosystem and combines the capabilities of Porous Flow with material objects that are able to allocate
spatially distributed data at element-resolution in the mesh. In this work, we first describe the workflow required to compile
85 a RHEA app, formulate a modelling problem and run a simulation. We then verify RHEA with one and two dimensional
analytical solutions, and propose a benchmark semi-analytical solution to validate RHEA's performance when sharp gradi-
ents are present. Finally, we apply RHEA to a complicated two dimensional problem with centimetre-scale heterogeneities
demonstrating its capabilities. We anticipate that our work will lay the foundation for accurate numerical modelling of hydro-
geomechanical problems allowing full spatial heterogeneity.

2 Governing equations

Modelling of coupled hydro-geomechanical processes requires solving the equations describing fluid flow in a deformable porous media. The coupled processes can be described physically in a representative elementary volume (REV) by a balance of fluid, mass and momentum, where local equilibrium of thermodynamics is assumed and macroscopic balance equations are considered to be the governing equations. In this section, the governing equations for hydro-geomechanical processes in fully saturated porous media with liquid fluid are presented on the basis of Biot's theory of consolidation. In the pore pressure formulation, the field variables are the liquid phase pressure p_f and the displacement vector $\boldsymbol{u}$. The material parameters can be spatially variable, but remain independent of time. Permeability and elastic parameters are described as tensors, whereas the Biot coefficient is a scalar.

Fluid flow within a deformable and fully saturated porous media is described by the continuity equation

$$\frac{1}{M}\frac{\partial p_f}{\partial t} + \alpha\frac{\partial \varepsilon_{kk}}{\partial t} + \nabla \cdot \boldsymbol{q}_d = Q_f \ , \tag{1}$$

where α is the Biot coefficient, ε_{kk} the volumetric strain, Q_f a fluid sink or source term and M is the Biot modulus of the porous media (the reciprocal of the storage coefficient). In Biot's consolidation theory, the Biot modulus is defined as

$$\frac{1}{M} = \frac{\phi}{K_f} + \frac{(\alpha - \phi)}{K_s} \ , \tag{2}$$

where ϕ, K_f, K_s represent the porosity, fluid and solid bulk modulus respectively. As Darcy flow is assumed, the fluid discharge $\boldsymbol{q}_d$ can be expressed as a momentum balance of the fluid like

$$\boldsymbol{q}_d = \phi(\boldsymbol{v}_f - \boldsymbol{v}_s) = -\frac{\boldsymbol{k}}{\mu_f}(\nabla p_f - \rho_f \boldsymbol{g}) \ , \tag{3}$$

where $\boldsymbol{v}_f$ and $\boldsymbol{v}_s$ are the fluid and solid matrix velocities respectively; $\boldsymbol{k}$ is the permeability tensor; μ_f is the dynamic viscosity of the fluid; ρ_f is the density of the fluid and $\boldsymbol{g}$ is the gravitational acceleration vector.

The mechanical model is defined via momentum balance in terms of the effective Cauchy stress tensor $\boldsymbol{\sigma}'(x,t)$ as

$$\nabla(\boldsymbol{\sigma}' - \alpha p_f \mathbb{I}) + \rho_b \boldsymbol{g} = 0 \ , \tag{4}$$

where $\mathbb{I}$ is the rank-two identity tensor. The mass of fluid per volume of porous media is expressed as the sum of the phases

$$\rho_b = \phi\rho_f + (1 - \phi)\rho_s \ , \tag{5}$$

where ρ_s is the solid density. The elastic strain can be expressed in terms of displacements with the relation

$$\boldsymbol{\varepsilon} = \frac{1}{2}(\nabla\boldsymbol{u} + \nabla^T\boldsymbol{u}) \ . \tag{6}$$

The effective stress is related to elastic strains by the generalized Hooke's law:

$$\boldsymbol{\varepsilon} = \varepsilon_{ij} = \mathbb{C}_{ijlk}\sigma'_{ij} \ , \tag{7}$$

where $\mathbb{C}_{ijkl}$ is the elastic compliance tensor.

Together, Eqs. 1 to 7 constitute the coupled system that represents hydro-geomechanical systems with linear elastic deformation.

3 Building RHEA

Real Heterogeneity App (RHEA) is an open-source simulation workflow and tool specifically developed to allow fully coupled numerical simulations in saturated porous media with spatially distributed heterogeneity in hydraulic and geomechanical properties. We built RHEA as a derivative of MOOSE, the massively parallel and open source FE simulation environment for coupled multi-physics processes (Gaston et al., 2009; Permann et al., 2020). MOOSE offers virtually unlimited simulation capabilities covering a wide spectrum of applications. This is based on a workflow where the end user does not need to know the details of the FE implementation. To achieve that, MOOSE utilises the libMesh library, a framework capable of manipulating multi-scale, multi-physics, parallel and mesh-adaptive FE simulations (Kirk et al., 2006). While the numerical methods, solvers and routines are executed by PETSc libraries (Balay et al., 2019), MOOSE is designed to allow the user to interact and control these two libraries without having to do any complex programming. Instead, the user frames the problem simply through an input file with unique syntax.

We found that learning how to perform numerical simulations based on the MOOSE framework is not a trivial task. Our aim is to further develop modelling capabilities while simplifying the complexity of the problem through an easy to follow workflow accompanied by a visual summary. The RHEA workflow can be summarised as follows:

Step 1 - RHEA compilation: The user creates the RHEA application following the structure outlined in Fig. 1. In other words, the user creates an executable file which is able to model fully coupled hydro-gemechanical systems in heterogenous media. We accomplished this by introducing material properties that can allocate data at each mesh element. Furthermore, we integrated the multi-physics of Section 2 to RHEA by adding the Porous Flow (Wilkins et al., 2020) and Tensor Mechanics modules that are part of the MOOSE framework. Once RHEA is downloaded, the user can access the necessary files to build RHEA, and can even access those files to modify the physics. This procedure is generic for any new MOOSE application. The core components of any MOOSE app such as RHEA are (Fig. 1):

Block 1 - Kernels: The *kernels* (or partial differential equation terms) describing the physics are implemented in their weak form (Jacob and Ted, 2007). In the MOOSE ecosystem, PDEs are represented by one simple line of code, this is highlighted with a cyan rectangle in Fig. 1. This straightforward way of describing complex multi-physics constitutes the most powerful feature of MOOSE.

Block 2 - Material properties: Values, including spatially-distributed values can be prescribed for each of the materials appearing in the *kernels*.

Block 3 - Kernel coupling: The user can couple different physics by including different *kernels* in its model, or by creating new *kernels*.

This dynamic procedure allows flexible creation of the RHEA application or any MOOSE-based application requiring minimal knowledge of C++ programming skills.

Step 2 - Preparation of material properties: The spatially distributed data is formatted to the structure required by the RHEA app compiled in Step 1. We implemented this with a custom Python script that imports and formats the original CSV or

VTK dataset into a RHEA-compatible data structure. Within RHEA, the hydro-geomechanical material properties are field properties which means that each value in the data set has to be allocated to a respective mesh element. Therefore, when the mesh is generated, the discretization has to match the number of data points of the data set. That way, each property value is represented within the simulation. Note that if it is not done correctly, RHEA may assign unwanted property values, since it uses a linear interpolation between neighbouring values.

Step 3 - Simulation setup: To define the numerical model, a RHEA script has to be created in the standard MOOSE syntax. The script consists of an array of systems that describe the mesh, physics, boundary conditions, numerical methods and outputs. A short example along with brief system descriptions is illustrated in Fig. 1. The blocks consist of MOOSE functions that are written and design in a generic manner and independently of the nature of the problem, this way the blocks can be recycled and reused. The spatially distributed material properties can be imported into the *Function* system and subsequently be stored in the *AuxVariable* system to be assigned as material property in the *Materials* block.

In summary, numerical simulations of hydro-geomechanical problems with spatially distributed material properties can be performed by calling RHEA's executable file (created in Step 1) using the simulation control script (created in Step 3) which contains the necessary instructions as well as reading in the spatially distributed material properties (created in Step 2).

4 Verifying RHEA

To test that RHEA accurately solves differential equations of Sect. 2 and that boundary conditions are correctly satisfied, four tests were developed. The proposed tests use predefined material properties that were imported into RHEA using the workflow presented in Sect. 3. The tests were designed to gradually build up complexity and cover the typical spectrum of consolidation problems. The four verification scenarios are described in the following subsections.

4.1 Terzaghi's problem

In the one dimensional consolidation problem, also known as Terzaghi's problem (Terzaghi, 1923), a single load q is applied at $t = 0$ on the top of a fully saturated homogeneous sample with the height L. The system is only drained at the top, where the pressure of the fluid is assumed to be $p = 0$ for $t > 0$. At the moment of loading, $t = 0$, the undrained compressibility of the solid increases the pressure of the sample. For $t > 0$, the system is allowed to drain and the consolidation processes begins.

In the absence of sources and sinks, Eq. 1 is reduced to the basic storage equation as

$$\frac{1}{M}\frac{\partial p_f}{\partial t} + \alpha\frac{\partial \varepsilon_{zz}}{\partial t} = \frac{k}{\gamma_f}\frac{\partial^2 p_f}{\partial z^2},\tag{8}$$

where the product $\rho_f \cdot g$ was written as γ_f and represents the volumetric weight of the fluid. Eq. 3 is used to couple the fluid discharge $\boldsymbol{q}_d$. From Hook's law, assuming one-dimensional deformation, the vertical strain equals the volume change

$$\frac{\partial \varepsilon_{zz}}{\partial t} = -m_v\frac{\partial \sigma'_{zz}}{\partial t} = -m_v\left(\frac{\partial \sigma_{zz}}{\partial t} - \alpha\frac{\partial p_f}{\partial t}\right),\tag{9}$$
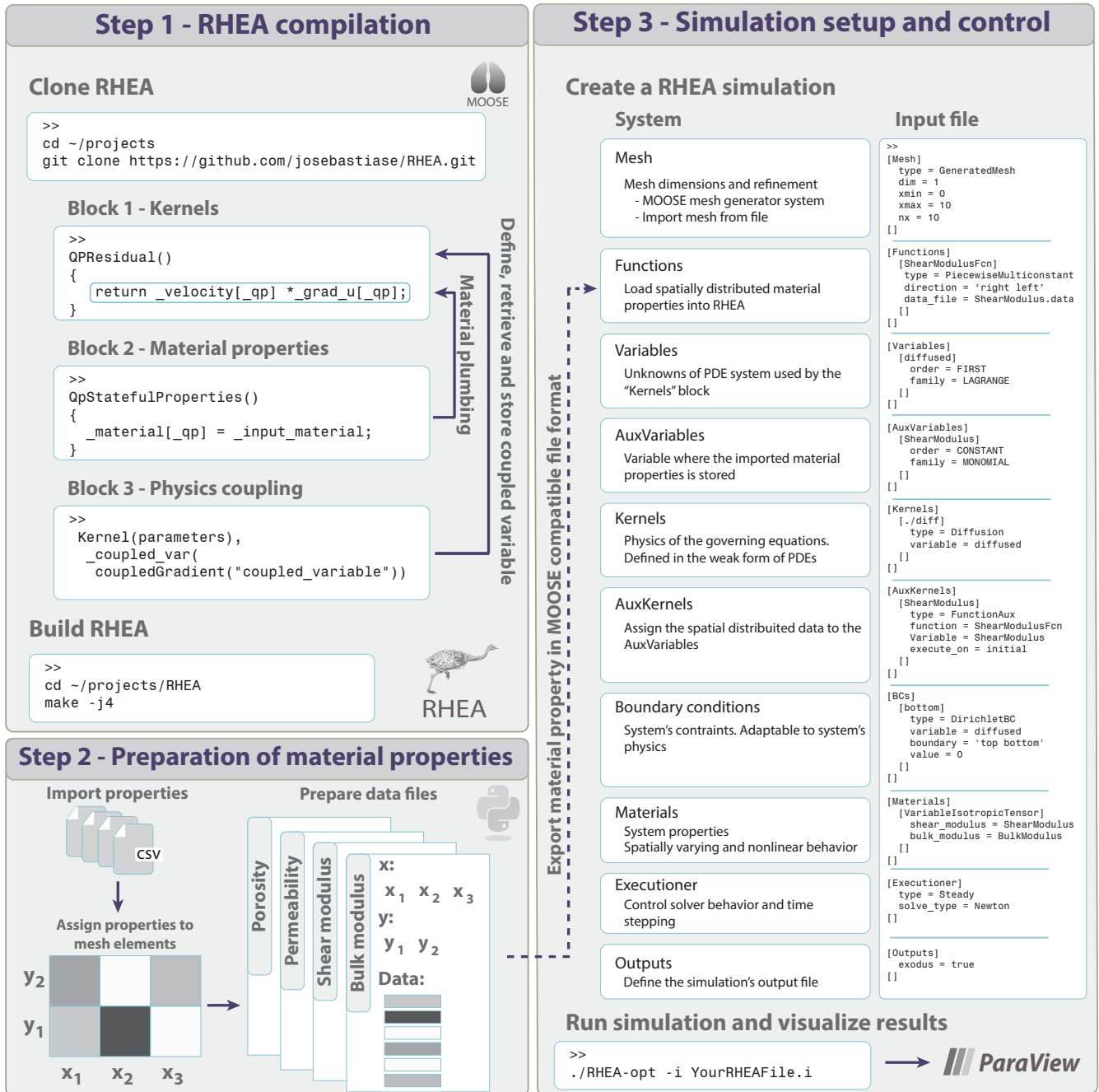
Figure 1. Visual illustration of the steps required to create RHEA, generate distributed material properties files and write a simulation script.

where m_v is the confined compressibility of the porous media

$$m_v = \frac{1}{K_s + (4/3)G_s} \tag{10}$$

and K_s and G_s are the bulk and shear moduli of the porous media respectively. Substituting Eq. 9 into the storage equation

185 (Eq. 8), the general differential equation for one dimensional consolidation is obtained:

$$\frac{\partial p_f}{\partial t} = \frac{\alpha m_v}{(1/M + \alpha^2 m_v)}\frac{\partial \sigma_{zz}}{\partial t} + \frac{k}{\gamma_f(1/M + \alpha^2 m_v)}\frac{\partial^2 p_f}{\partial z^2} \tag{11}$$

For $t > 0$, the total load q is kept constant and the total stress σ_{zz} is also constant. Consequently, Eq. 11 reduces to

$$t > 0 : \frac{\partial p_f}{\partial t} = \frac{k}{\gamma_f(1/M + \alpha^2 m_v)}\frac{\partial^2 p_f}{\partial z^2}. \tag{12}$$

Since the system is undrained at $t = 0$, the initial condition can be established from Eq. 11 as

190 $$t = 0 : p_f = p_0 = \frac{\alpha m_v}{(1/M + \alpha^2 m_v)}q. \tag{13}$$

The boundary conditions at the top and bottom of the sample are

$$t > 0, z = L : p_f = 0 \tag{14}$$

and

$$t > 0, z = 0 : \frac{\partial p_f}{\partial z} = 0. \tag{15}$$

195 The analytical solution of the problem is well known and reads (Wang, 2017; Cheng, 2016; Verruijt, 2018)

$$\frac{p_f}{p_0} = \frac{4}{\pi}\sum_{k=1}^{\infty}\frac{(-1)^{k-1}}{2k-1}\cos\left[(2k-1)\frac{\pi}{2}\frac{z}{L}\right]\exp\left[-(2k-1)^2\frac{\pi^2}{4}\frac{kt}{\gamma_f(1/M + \alpha^2 m_v)L^2}\right]. \tag{16}$$

For this example, the height of the sample was set to $100\,\mathrm{m}$, the hydraulic conductivity is $1 \cdot 10^{-4}\,\mathrm{m/s}$, the porosity is 0.2, the Biot coefficient is 0.9, the bulk modulus is $8.40 \cdot 10^7\,\mathrm{Pa}$ and the shear modulus is $6.25 \cdot 10^7\,\mathrm{Pa}$. The performance and consistency of RHEA on the consolidation problem is shown as pore pressure versus depth profiles at discrete times in Fig. 2a.

200 A comparison of the analytical and RHEA's solution reveals excellent agreement, thereby verifying the numerical solution.

4.2 Layered Terzaghi's problem

The objective of this test is to investigate the performance of RHEA when heterogeneity and sharp gradients are present. The consolidation experiment of the previous section is performed on a sample with multiple layers of contrasting properties. For simplicity, porosity and mechanical parameters are assumed homogeneous. Since the total load q is constant for $t > 0$, Eq. 11

205 reduces to Eq. 12 across n layers as follows

$$t > 0 : \frac{\partial p_{fi}}{\partial t} = \frac{k_i}{\gamma_f(1/M + \alpha^2 m_v)}\frac{\partial^2 p_{fi}}{\partial z^2}, \quad i \in [1, n], \tag{17}$$

which describes the consolidation in each layer. Here, $z_{i-1} \le z \le z_i$ is the depth of the sample, p_{fi} and k_i are the fluid pressure and permeability of the solid in each layer i, respectively. The contact between layers is assumed to be perfect, i.e. the boundary conditions at the layers is represented by equivalent matching fluid pressure as

210 $$t > 0, z = z_i : k_i \frac{\partial p_{fi}}{\partial z} = k_{i+1}\frac{\partial p_{fi+1}}{\partial z}. \tag{18}$$

The sample is drained at the top, whereas the bottom remains undrained

$$t > 0, z = z_0 = H : p_f = 0 \tag{19}$$

and

$$t > 0, z = z_n = 0 : \frac{\partial p_f}{\partial z} = 0. \tag{20}$$

215   The fluid pressure produced by the external load starts to dissipate when $t > 0$, but at different rates depending on the consolidation coefficient of the layer. The height of the sample is $100\,\mathrm{m}$ and 10 layers are equally distributed along the sample with $10\,\mathrm{m}$ height. To represent sharp gradients, the selected hydraulic conductivities have four orders of magnitude difference between layers, $1 \cdot 10^{-4}\,\mathrm{m/s}$ and $1 \cdot 10^{-8}\,\mathrm{m/s}$. The high and low permeability layers are alternating. The porosity is set to 0.2, the Biot coefficient is 0.9, the bulk modulus is $8.40 \cdot 10^7\,\mathrm{Pa}$ and the shear modulus is $6.25 \cdot 10^7\,\mathrm{Pa}$.

220   A step-by-step semi-analytical solution of the diffusion problem in a layered sample was derived by Hickson et al. (2009). To solve this problem in RHEA, a mesh of 100 elements was used with a time step of $1 \cdot 10^4$ s. A comparison between the analytical solution and RHEA's numerical simulation is shown in Fig. 2b. In the layers with high hydraulic conductivity, the consolidation process occurs rapidly leading to faster pore pressure dissipation (vertical pore pressure profile), and therefore also faster water movement. In contrast, the consolidation process is slower in the low conductivity layers with slower pore

225   pressure dissipation and water movement.

4.3   Plane strain consolidation

To evaluate the performance of RHEA for two-dimensional heterogeneity, a consolidation problem with plane strain is developed. The two-dimensional consolidation caused by a uniform load over a circular homogeneous area can be represented by the storage equation (Eq. 1) in two dimensional case as

230    $$\frac{1}{M}\frac{\partial p_f}{\partial t} + \alpha\frac{\partial \varepsilon}{\partial t} = \frac{k}{\gamma_f}\left(\frac{\partial^2 p_f}{\partial x^2} + \frac{\partial^2 p_f}{\partial z^2}\right) \tag{21}$$

where ε represents the volumetric strain. Including two equilibrium equations, in terms of total stress, as

$$\frac{\partial \sigma_{xx}}{\partial x} + \frac{\partial \sigma_{zx}}{\partial z} = 0 \tag{22}$$

and

$$\frac{\partial \sigma_{xz}}{\partial x} + \frac{\partial \sigma_{zz}}{\partial z} = 0. \tag{23}$$

235   The total stress is related to the effective stress through

$$\sigma_{xx} = \sigma'_{xx} + \alpha p \qquad \sigma_{xz} = \sigma'_{xz} \tag{24}$$

and

$$\sigma_{zz} = \sigma'_{zz} + \alpha p \qquad \sigma_{zx} = \sigma'_{zx}. \tag{25}$$
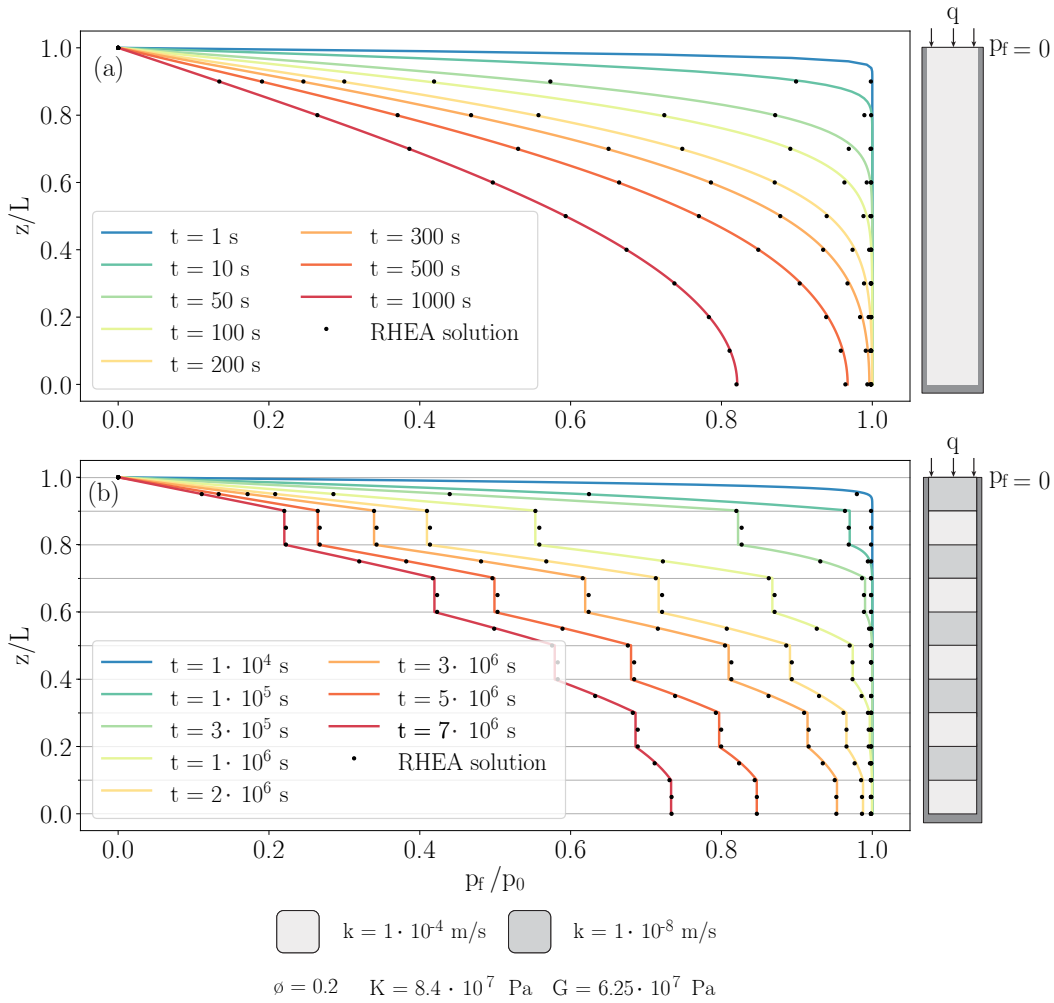
Figure 2. Comparison of analytical and numerical solution of the one dimensional consolidation problem obtained in a sample of $100\,\text{m}$. (a) Homogeneous case (b) Heterogeneous case. The lines represent the analytical solution whereas the dots represent the RHEA solution.

The analytical solution can be found by expressing the equilibrium Eq. 22 and Eq. 23 in terms of the displacement components

240   u_x and u_z using Hooke's law as

$$\sigma'_{xx} = -\left(K_s - \frac{2}{3}G_s\right)\varepsilon - 2G_s\frac{\partial u_x}{\partial x} \tag{26}$$

and

$$\sigma'_{zz} = -\left(K_s - \frac{2}{3}G_s\right)\varepsilon - 2G_s\frac{\partial u_z}{\partial z} \tag{27}$$

and

$$\sigma'_{xz} = \sigma'_{zx} = -G_s \left(\frac{\partial u_z}{\partial x} + \frac{\partial u_x}{\partial z} \right). \tag{28}$$

Here, the assumed plane strain is the y axis, i.e. $u_y = 0$. Replacing Hooke's law in plane strain (Eq. 26 to 28) with the effective stress balance (Eq. 22 and Eq. 23 combined with Eq. 24 and Eq. 25) leads to a complete system of equations as

$$\left(K_s + \frac{1}{3}G_s \right) \frac{\partial \varepsilon}{\partial x} + G_s \nabla^2 u_x - \alpha \frac{\partial p_f}{\partial x} = 0 \tag{29}$$

and

$$\left(K_s + \frac{1}{3}G_s \right) \frac{\partial \varepsilon}{\partial z} + G_s \nabla^2 u_z - \alpha \frac{\partial p_f}{\partial z} = 0, \tag{30}$$

where the elastic strain is

$$\varepsilon = \frac{\partial u_x}{\partial x} + \frac{\partial u_z}{\partial z}. \tag{31}$$

The boundary conditions are represented by a constant load in an area of width $2a$, applied at $t = 0$. The system is allowed to drain for $t > 0$ as

$$t > 0, \ z = 0: \ p_f = 0 \tag{32}$$

and

$$t > 0, \ z = 0: \ \sigma_{zz} = \begin{cases} q, & |x| < a \\ 0, & |x| > a \end{cases} \tag{33}$$

and

$$t > 0, \ z = 0: \ \sigma_{xz} = 0. \tag{34}$$

When the sample is loaded, a confined pore pressure in generated which starts to drain instantaneously through the borders of the system. A semi analytical solution in the Fourier domain and Laplace transform for the given equation system and boundary conditions is presented in Verruijt (2013). The height and the width of the sample are $10\,\mathrm{m}$. The load is applied on the surface of the sample between -1 and $1\,\mathrm{m}$. The hydraulic conductivity is $1 \cdot 10^{-5}\,\mathrm{m/s}$, the porosity is 0.2, the Biot coefficient is 0.9, the bulk modulus is $8.40 \cdot 10^7\,\mathrm{Pa}$ and the shear modulus is $6.25 \cdot 10^7\,\mathrm{Pa}$. To solve this problem, a coarse mesh was defined, and MOOSE's native mesh adaptivity system was employed to automatically generate a finer resolution in areas where the pore pressure gradients are steep. This significantly reduces the computational time when compared with using a fine mesh throughout.

The results are illustrated in two figures, Fig. 3a shows a cross section of the sample as contour plot. Figure 3b shows a pore pressure profile with depth at the center of the sample $x = 0\,\mathrm{m}$. Excellent agreement between the analytical solution and the simulated solution by RHEA is observed.
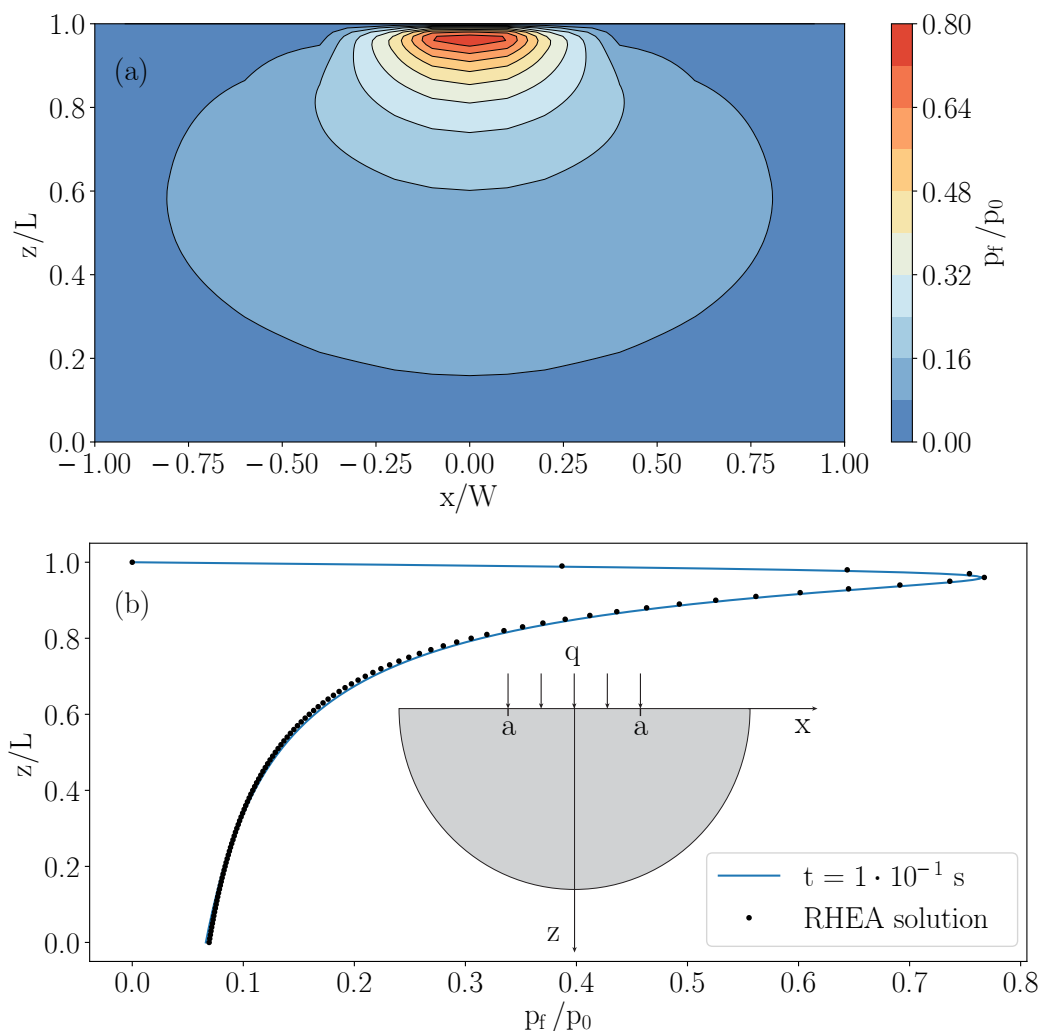
Figure 3. The solution of the consolidation problem in plane strain by RHEA is shown in a sample $10\,\mathrm{m}$ wide and $10\,\mathrm{m}$ of height. (a) Contour plot of the solution at time $1 \cdot 10^{-2}$ s. (b) A comparison of the semi-analytical solution (continuous line) and the RHEA solution (dotted line). The differences in pore pressure between both approaches is due to the assumption of an infinite domain in the analytical solution which is not feasible to replicate the latter with RHEA.

4.4 Modelling realistic geology

The last example aims to study and illustrate the performance of RHEA's with a real data set. The 2D consolidation problem was solved with RHEA, integrating the multi-facies realizations and material properties of the Herten analog (Bayer et al., 2015).

4.4.1 Herten aquifer dataset description

Realistic modelling relies not only on accurate data concerning material parameters, but also on appropriate spatial distribution of such parameters (Houben et al., 2018; Irvine et al., 2015; Kalbus et al., 2009). Typically, distributed material parameters are generated by stochastic random fields based on an *a priori* statistical distribution (Vanmarcke et al., 1986). Although random fields have proven to be useful, they do not capture the usual continuity of material parameters (Strebelle, 2002). Consequently, the use of high resolution data, such as "aquifer analogs", is preferred (Alexander, 1993; Zappa et al., 2006). Aquifer analogs consist of centimeter-resolution data obtained from detailed investigation of geological formations at outcrops. Although aquifer analogs are rare, they have been widely used in different subsurface fields (Höyng et al., 2015; Beaujean et al., 2014; Finkel et al., 2016). The Herten analog is a well-known and rigorously generated 2D outcrop (Bayer et al., 2015). It consists of a fluvial braided river deposit from the south east of Germany, which represents one of the most important drinking water resources in central Europe. Its architecture consists of sedimentary facies, and its body of unconsolidated gravel and well sorted sand. The dimensions of the 2D outcrop are 16 m wide by 7 m high, and features horizontal and vertical data resolution of 5 cm for hydraulic conductivity and porosity. Hence, the 2D cross-section has a total of 4480 measurements points. The corresponding hydraulic conductivity k, ranges from $6.0 \cdot 10^{-7}$ m/s to $1.3 \cdot 10^{-1}$ m/s, and porosity ϕ, from 0.17 to 0.36 (Fig. 4a). To represent spatial distribution of mechanical properties, typical values of bulk and shear moduli for gravel and sand were assumed to be linearly correlated with the porosity of the aquifer: similar trends have been reported in previous studies (Mondol et al., 2008; Hardin and Kalinski, 2005; Hicher, 1996). Representative geomechanical moduli can be found in soil mechanics literature as shown in Table 1. The elastic tensor is assumed isotropic in this example, hence elastic moduli are related via (Wang, 2017; Cheng, 2016)

$$
\begin{aligned}
K_s &= \frac{E_s}{3(1-2\nu_s)} \\
G_s &= \frac{E_s}{2(1+\nu_s)} \, ,
\end{aligned}
\tag{35}
$$

where E_s and ν_s denote the Young's modulus and Poisson's ratio of the solid material respectively. The result is that the bulk moduli vary between $6.7 \cdot 10^7$ Pa and $1.7 \cdot 10^8$ Pa, whereas the shear moduli range between $3.0 \cdot 10^7$ Pa and $3.5 \cdot 10^8$ Pa, as shown in Fig. 4a. RHEA does not require the mechanical moduli to be related to the hydraulic properties in the way we have described in this particular example.

4.4.2 Problem and model description

The two dimensional consolidation is described by Eqs. 21, 29 and 30. A constant load at the top of the sample is applied at $t > 0$, which generates a confined pore pressure. After that, the system is allowed to drain through the top boundary and is subjected to the normal stress. The sample's bottom and sides are impermeable to the fluid, and subject to roller boundary conditions.

For this simulation, a quadrilateral mesh was generated with the mesh generator system of MOOSE. The mesh has $44\,800$ elements and $44\,940$ nodes, which matches the data set resolution. Since the material properties of the data set differs in orders

Material	Young's modulus (MPa)	Poisson's ratio (-)	Reference
Loose gravel	48 - 148	-	(Subramanian, 2011)
Dense gravel	96 - 192	-	(Subramanian, 2011)
Gravel	50 - 100	0.3 - 0.35	(Look, 2014)
Sand and gravel	69.0 - 172.5	0.15 - 0.35	(Das, 2019)
Gravel	68.9 - 413.7	0.4	(Xu, 2016)
Dense sand	-	0.3 - 0.4	(Lade, 2001)
Loose sand	-	0.1 - 0.3	(Lade, 2001)
Gravel	-	0.1 - 0.4	(Kulhawy and Mayne, 1990)

Table 1. Typical elastic properties of sand and gravel.

of magnitude, the mesh adaptivity system of MOOSE was used to ensure accurate results. At each time step the 30% of elements with the highest porepressure gradient were refined, which reduces the local error at contrasting facies. Hence the mesh is refined in each time step. At the end of the simulation, the number of nodes had grown to $708\,548$ and the number of elements to $631\,615$.

4.4.3 Simulation results

The pore pressure profiles depicted in Fig. 5 illustrate how the physical heterogeneity of the cross-bedded data set strongly influences the fluid flow through the sample. The effect of the centimeter resolution of the data set can be studied when the initial load is applied at $t = 0$. Since the sample is not yet allowed to drain, confined porepressure is generated which depends on the geomechanical characteristics of the sand and gravel. In facies where the soil is highly compressible, the generated pore pressure is also relatively high since the total load is shared between the the fluid and the soil. In contrast, in facies that have higher elastic moduli values the confined pore pressure is relatively low. This effect is nicely shown in Fig. 5a. At time $t > 0$ the top of the sample is allowed to drain. The effect of the highly permeable units made of poorly sorted and well sorted gravel is shown in Fig. 5b. The top facie of the aquifer consists of a highly permeable soil ($k = 1.3 \cdot 10^{-1}$ m/s), which is divided by a thin low permeable layer ($k = 6.1 \cdot 10^{-5}$ m/s), the latter causes contrasting pore pressure profiles. Similar permeability effects have been discussed before (Choo and Lee, 2018; Peng et al., 2017; Kadeethum et al., 2019). The influence of the temporal and spatial scales on the consolidation process is shown in Fig. 5c and 5d. It can be observed that the process occurs rather quickly and is strongly influenced by the low permeability facies. This example demonstrates that RHEA can solve complex and realistic heterogenous hydro-geomechanical coupled problems.

(a)

k [m/s]	$1.3 \cdot 10^{-1}$	$9.5 \cdot 10^{-2}$	$2.6 \cdot 10^{-2}$	$2.3 \cdot 10^{-3}$	$1.4 \cdot 10^{-4}$	$2.3 \cdot 10^{-4}$	$2.5 \cdot 10^{-4}$	$4.3 \cdot 10^{-5}$	$6.1 \cdot 10^{-5}$	$6.0 \cdot 10^{-7}$
ø [-]	0.26	0.23	0.26	0.27	0.36	0.15	0.17	0.22	0.13	0.20
K $[\mathrm{Pa} \cdot 10^{7}]$	10.2	9.65	10.2	10.4	13.3	8.55	8.78	9.48	8.33	9.18
G $[\mathrm{Pa} \cdot 10^{7}]$	3.67	3.45	3.54	3.75	3.85	3.25	3.29	3.42	2.85	3.29

(b)

Automatic mesh refinement

$t = 0.0 \ \mathrm{s}$ $\qquad$ $t = 1.0 \cdot 10^{-3} \ \mathrm{s}$ $\qquad$ $t = 1.0 \cdot 10^{-2} \ \mathrm{s}$ $\qquad$ $t = 1.0 \cdot 10^{-1} \ \mathrm{s}$
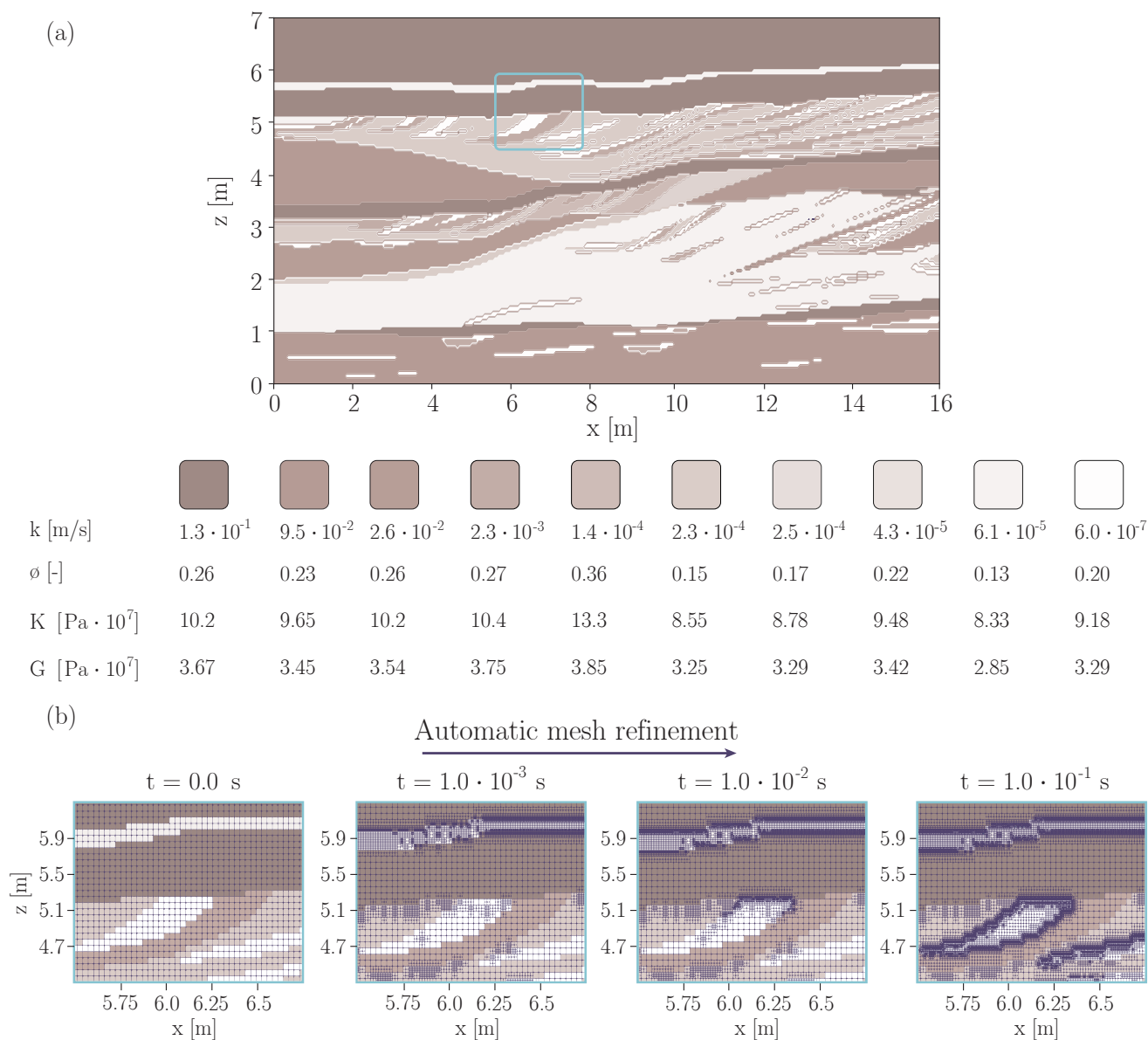
Figure 4. Facie architecture and properties of the Herten aquifer analog. (a) Color scale of the hydro-geomechanical properties of the aquifer imported to RHEA. (b) Shows the mesh discretization and its dynamic evolution when the mesh adaptivity system is activated. The time evolution is shown from left to right.
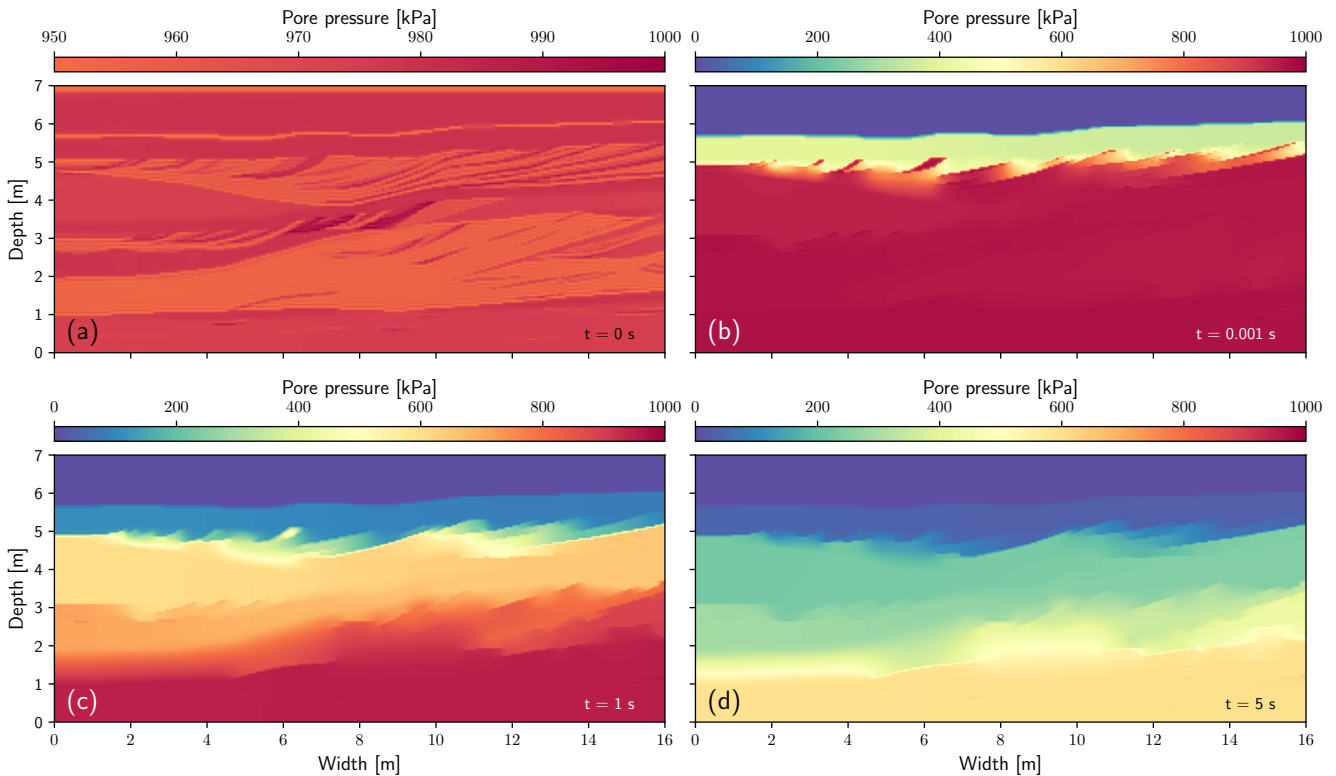
Figure 5. Sequence of snapshots of the consolidation process and pore pressure variation in the aquifer with time. (a) Displays the initial condition of the simulation. (b) Snapshot at time $1 \cdot 10^{-3}$ s. (c) Snapshot at time 1 s. (d) Snapshot at time 5 s. Note that (a) uses a different colour range to highlight the small variations in pore pressure.

5 RHEA's potential

325 In this paper we develop and verify Real HEterogeneity App (RHEA): a numerical simulation tool that allows fully coupled numerical modelling of hydro-geomechanical systems. Moreover, RHEA can easily include full heterogeneity of parameters as occurs in real subsurface systems. RHEA is based on the powerful Multiphysics Object-Oriented Simulation Environment (MOOSE) open source framework. Furthermore, we provide an easy-to-understand workflow which explains how to compile the application and run a customised numerical simulation. Despite its simplicity, the workflow combines all the technical

330 advantages provided by MOOSE and its well established framework. The latter allows the development and use of state-of-the-art and massively scalable applications backed by the unconditional support of a growing community.

Beyond unlocking the ability to include full heterogeneity of hydro-geomechanical parameters in simulations, our contribution provides examples to verify future numerical codes. Additionally, a semi-analytical benchmark problem is proposed to verify the performance of numerical code when heterogeneity and sharp gradients are present.

335   Our example simulations illustrate that the subsurface hydro-geomechanical properties, in particular permeability (or transmissivity), plays a key role in the consolidation process. Although this insight is valuable, it can lead to an oversimplification when models assume transmissivity varies heterogeneously while mechanical parameters are assumed homogeneous. This approach can lead to biased results in systems where different geologic formations are present. For example, this is the case when excessive groundwater extraction causes the depletion of a confined aquifer producing irreversible land surface subsidence.

340 Geological heterogeneities can play a significant role when estimating surface deformation.

    RHEA has the potential to advance our understanding of real world systems that have previously been oversimplified. Further, RHEA offers the integration of high resolution data set with sophisticated numerical implementations. Potential numerical instabilities caused by highly heterogeneous systems (i.e. settings with sharp gradients) are handled automatically by combining adaptive meshing capabilities with implicit time stepping.

345   Our current work focuses on hydro-geomechanical coupling of heterogeneous systems. However, RHEA could potentially be extended to include also thermal processes. While it would allow fully coupled simulations of thermal-hydraulic-mechanical (THM) systems including spatially distributed heterogeneities, verification will require the development of more advanced analytical solutions, a task that however is beyond the scope of this contribution.

Code and data availability. The RHEA code is available in the GitHub repository https://github.com/josebastiase/RHEA. Verification and
350 examples included in this work are found in the examples folder of the GitHub repository. The Herten analogue data set is available on https://doi.pangaea.de/10.1594/PANGAEA.844167.

Author contributions. JMBE developed RHEA, the analytical solutions used for verification, made the figures and tables and wrote the first manuscript draft. GCR closely supervised JMBE. AW provided JMBE with technical support. PB reviewed the manuscript and provided suggestions.

355 *Competing interests.* The authors declare that they have no competing interests.

Acknowledgements. This project has received funding from the German Research Council (DFG) grant agreement number 424795466.

References

Alexander, J.: A discussion on the use of analogues for reservoir geology, Geological Society, London, Special Publications, 69, 175–194, 1993.

360   Alnæs, M., Blechta, J., Hake, J., Johansson, A., Kehlet, B., Logg, A., Richardson, C., Ring, J., Rognes, M. E., and Wells, G. N.: The FEniCS project version 1.5, Archive of Numerical Software, 3, 2015.

Atkinson, B. K.: Fracture mechanics of rock, Elsevier, 2015.

Balay, S., Abhyankar, S., Adams, M., Brown, J., Brune, P., Buschelman, K., Dalcin, L., Dener, A., Eijkhout, V., Gropp, W., et al.: PETSc users manual, 2019.

365   Bayer, P., Comunian, A., Höyng, D., and Mariethoz, G.: High resolution multi-facies realizations of sedimentary reservoir and aquifer analogs, Scientific data, 2, 1–10, 2015.

Bear, J. and Verruijt, A.: Modeling groundwater flow and pollution, vol. 2, Springer Science & Business Media, 1987.

Beaujean, J., Lemieux, J.-M., Dassargues, A., Therrien, R., and Brouyère, S.: Physically based groundwater vulnerability assessment using sensitivity analysis methods, Groundwater, 52, 864–874, 2014.

370   Beck, M., Rinaldi, A., Flemisch, B., and Class, H.: Accuracy of fully coupled and sequential approaches for modeling hydro-and geomechanical processes, Computational Geosciences, 24, 1707–1723, 2020.

Berre, I., Doster, F., and Keilegavlen, E.: Flow in fractured porous media: A review of conceptual models and discretization approaches, Transport in Porous Media, 130, 215–236, 2019.

Biot, M. A.: General theory of three-dimensional consolidation, Journal of applied physics, 12, 155–164, 1941.

375   Birdsell, D. T. and Saar, M. O.: Modeling ground surface deformation at the Swiss HEATSTORE underground thermal energy storage sites, in: World Geothermal Congress (2020)(online), ETH Zurich, Institute of Geophysics, 2020.

Birkholzer, J. T., Tsang, C.-F., Bond, A. E., Hudson, J. A., Jing, L., and Stephansson, O.: 25 years of DECOVALEX-Scientific advances and lessons learned from an international research collaboration in coupled subsurface processes, International Journal of Rock Mechanics and Mining Sciences, 122, 103 995, 2019.

380   Blum, P., Mackay, R., Riley, M., and Knight, J.: Performance assessment of a nuclear waste repository: upscaling coupled hydro-mechanical properties for far-field transport analysis, International Journal of Rock Mechanics and Mining Sciences, 42, 781–792, 2005.

Blum, P., Mackay, R., and Riley, M. S.: Stochastic simulations of regional scale advective transport in fractured rock masses using block upscaled hydro-mechanical rock property data, Journal of Hydrology, 369, 318–325, 2009.

Boone, T. J. and Ingraffea, A. R.: A numerical procedure for simulation of hydraulically-driven fracture propagation in poroelastic media,
385   International Journal for Numerical and Analytical Methods in Geomechanics, 14, 27–47, 1990.

Cacace, M. and Jacquey, A. B.: Flexible parallel implicit modelling of coupled thermal–hydraulic–mechanical processes in fractured rocks, Solid Earth, 8, 921–941, 2017.

Cheng, A. H.-D.: Poroelasticity, vol. 27, Springer, 2016.

Choo, J. and Lee, S.: Enriched Galerkin finite elements for coupled poromechanics with local mass conservation, Computer Methods in
390   Applied Mechanics and Engineering, 341, 311–332, 2018.

Cundall, P. A. and Hart, R. D.: Numerical modeling of discontinua, in: Analysis and design methods, pp. 231–243, Elsevier, 1993.

Das, B. M.: Advanced soil mechanics, Crc Press, 2019.

Eaton, T. T.: On the importance of geological heterogeneity for flow simulation, Sedimentary Geology, 184, 187–201, 2006.

Finkel, M., Grathwohl, P., and Cirpka, O. A.: A travel time-based approach to model kinetic sorption in highly heterogeneous porous media
395   via reactive hydrofacies, Water Resources Research, 52, 9390–9411, 2016.

Freymark, J., Bott, J., Cacace, M., Ziegler, M., and Scheck-Wenderoth, M.: Influence of the main border faults on the 3d hydraulic field of
the central Upper Rhine Graben, Geofluids, 2019, 2019.

Gariano, S. L. and Guzzetti, F.: Landslides in a changing climate, Earth-Science Reviews, 162, 227–252, 2016.

Gaston, D., Newman, C., Hansen, G., and Lebrun-Grandie, D.: MOOSE: A parallel computational framework for coupled systems of non-
400   linear equations, Nuclear Engineering and Design, 239, 1768–1778, 2009.

Green, C., Wilkins, A., La Force, T., and Ennis-King, J.: Community code for simulating CO2 storage: Modelling multiphase flow with
coupled geomechanics and geochemistry using the open-source multiphysics framework MOOSE, in: 14th Greenhouse Gas Control
Technologies Conference Melbourne, pp. 21–26, 2018.

Grigoli, F., Cesca, S., Priolo, E., Rinaldi, A. P., Clinton, J. F., Stabile, T. A., Dost, B., Fernandez, M. G., Wiemer, S., and Dahm, T.: Current
405   challenges in monitoring, discrimination, and management of induced seismicity related to underground industrial activities: A European
perspective, Reviews of Geophysics, 55, 310–340, 2017.

Haagenson, R., Rajaram, H., and Allen, J.: A generalized poroelastic model using FEniCS with insights into the Noordbergum effect,
Computers & Geosciences, 135, 104 399, 2020.

Haque, U., Blum, P., Da Silva, P. F., Andersen, P., Pilz, J., Chalov, S. R., Malet, J.-P., Auflič, M. J., Andres, N., Poyiadji, E., et al.: Fatal
410   landslides in Europe, Landslides, 13, 1545–1554, 2016.

Hardin, B. O. and Kalinski, M. E.: Estimating the shear modulus of gravelly soils, Journal of geotechnical and geoenvironmental engineering,
131, 867–875, 2005.

Hein, P., Kolditz, O., Görke, U.-J., Bucher, A., and Shao, H.: A numerical study on the sustainability and efficiency of borehole heat exchanger
coupled ground source heat pump systems, Applied Thermal Engineering, 100, 421–433, 2016.

415   Herron, N., Peeters, L., Crosbie, R., Marvanek, S., Ramage, A., Rachakonda, P., and Wilkins, A.: Groundwater Numerical Modelling for the
Hunter Subregion. Product 2.6. 2 for the Hunter Subregion from the Northern Sydney Basin Bioregional Assessment, 2018.

Hicher, P.-Y.: Elastic properties of soils, Journal of Geotechnical Engineering, 122, 641–648, 1996.

Hickson, R., Barry, S., and Mercer, G.: Critical times in multilayer diffusion. Part 1: Exact solutions, International Journal of Heat and Mass
Transfer, 52, 5776–5783, 2009.

420   Holzbecher, E.: Poroelasticity benchmarking for FEM on analytical solutions, in: Excerpt from the Proceedings of the COMSOL Conference
Rotterdam, pp. 1–7, 2013.

Houben, G. J., Stoeckl, L., Mariner, K. E., and Choudhury, A. S.: The influence of heterogeneity on coastal groundwater flow-physical and
numerical modeling of fringing reefs, dykes and structured conductivity fields, Advances in Water Resources, 113, 155–166, 2018.

Höyng, D., Prommer, H., Blum, P., Grathwohl, P., and D'Affonseca, F. M.: Evolution of carbon isotope signatures during reactive transport
425   of hydrocarbons in heterogeneous aquifers, Journal of contaminant hydrology, 174, 10–27, 2015.

Irvine, D. J., Cranswick, R. H., Simmons, C. T., Shanafield, M. A., and Lautz, L. K.: The effect of streambed heterogeneity on groundwater-
surface water exchange fluxes inferred from temperature time series, Water Resources Research, 51, 198–212, 2015.

Jacob, F. and Ted, B.: A first course in finite elements, Wiley, 2007.

Kadeethum, T., Nick, H., Lee, S., Richardson, C., Salimzadeh, S., Ballarin, F., et al.: A Novel Enriched Galerkin Method for Modelling
430   Coupled Mechanical Deformation in Heterogeneous Porous Media, in: 53rd US Rock Mechanics/Geomechanics Symposium, American
Rock Mechanics Association, 2019.

Kalbus, E., Schmidt, C., Molson, J., Reinstorf, F., and Schirmer, M.: Influence of aquifer and streambed heterogeneity on the distribution of groundwater discharge., Hydrology & Earth System Sciences, 13, 2009.

Keilegavlen, E., Fumagalli, A., Berge, R., Stefansson, I., and Berre, I.: PorePy: an open-source simulation tool for flow and transport in deformable fractured rocks, arXiv preprint arXiv:1712.00460, 2017.

Kim, J., Tchelepi, H. A., and Juanes, R.: Stability and convergence of sequential methods for coupled flow and geomechanics: Fixed-stress and fixed-strain splits, Computer Methods in Applied Mechanics and Engineering, 200, 1591–1606, 2011.

Kirk, B. S., Peterson, J. W., Stogner, R. H., and Carey, G. F.: libMesh: a C++ library for parallel adaptive mesh refinement/coarsening simulations, Engineering with Computers, 22, 237–254, 2006.

Kolditz, O., Bauer, S., Bilke, L., Böttcher, N., Delfs, J.-O., Fischer, T., Görke, U. J., Kalbacher, T., Kosakowski, G., McDermott, C., et al.: OpenGeoSys: an open-source initiative for numerical simulation of thermo-hydro-mechanical/chemical (THM/C) processes in porous media, Environmental Earth Sciences, 67, 589–599, 2012.

Kulhawy, F. H. and Mayne, P. W.: Manual on estimating soil properties for foundation design, Tech. rep., Electric Power Research Inst., Palo Alto, CA (USA); Cornell Univ., Ithaca, NY (USA), 1990.

Lade, P. V.: Engineering properties of soils and typical correlations, in: Geotechnical and geoenvironmental engineering handbook, pp. 43–67, Springer, 2001.

Lecampion, B., Bunger, A., and Zhang, X.: Numerical methods for hydraulic fracture propagation: a review of recent trends, Journal of natural gas science and engineering, 49, 66–83, 2018.

Lee, J., Kim, K.-I., Min, K.-B., and Rutqvist, J.: TOUGH-UDEC: A simulator for coupled multiphase fluid flows, heat transfers and discontinuous deformations in fractured porous media, Computers & Geosciences, 126, 120–130, 2019.

Lei, H., Xu, T., and Jin, G.: TOUGH2Biot–A simulator for coupled thermal–hydrodynamic–mechanical processes in subsurface flow systems: Application to CO2 geological storage and geothermal development, Computers & Geosciences, 77, 8–19, 2015.

Look, B. G.: Handbook of geotechnical investigation and design tables, CRC Press, 2014.

McMillan, T. C., Rau, G. C., Timms, W. A., and Andersen, M. S.: Utilizing the impact of Earth and atmospheric tides on groundwater systems: A review reveals the future potential, Reviews of Geophysics, 57, 281–315, 2019.

Mondol, N. H., Jahren, J., Bjørlykke, K., and Brevik, I.: Elastic properties of clay minerals, The Leading Edge, 27, 758–770, 2008.

Morris, J. P., Rubin, M., Block, G., and Bonner, M.: Simulations of fracture and fragmentation of geologic materials using combined FEM/DEM analysis, International Journal of Impact Engineering, 33, 463–473, 2006.

Nghiem, L., Sammon, P., Grabenstetter, J., Ohkuma, H., et al.: Modeling CO2 storage in aquifers with a fully-coupled geochemical EOS compositional simulator, in: SPE/DOE symposium on improved oil recovery, Society of Petroleum Engineers, 2004.

Pandey, S., Vishal, V., and Chaudhuri, A.: Geothermal reservoir modeling in a coupled thermo-hydro-mechanical-chemical approach: A review, Earth-Science Reviews, 185, 1157–1169, 2018.

Peng, S.: Surface Subsidence Engineering: Theory and Practice, CSIRO PUBLISHING, 2020.

Peng, X., Zhang, L., Jeng, D., Chen, L., Liao, C., and Yang, H.: Effects of cross-correlated multiple spatially random soil properties on wave-induced oscillatory seabed response, Applied Ocean Research, 62, 57–69, 2017.

Permann, C. J., Gaston, D. R., Andrš, D., Carlsen, R. W., Kong, F., Lindsay, A. D., Miller, J. M., Peterson, J. W., Slaughter, A. E., Stogner, R. H., et al.: MOOSE: Enabling massively parallel multiphysics simulation, SoftwareX, 11, 100 430, 2020.

Pham, H. T., Rühaak, W., Schuster, V., and Sass, I.: Fully hydro-mechanical coupled Plug-in (SUB+) in FEFLOW for analysis of land subsidence due to groundwater extraction, SoftwareX, 9, 15–19, 2019.

470 Pruess, K., Oldenburg, C. M., and Moridis, G.: TOUGH2 user's guide version 2, Tech. rep., Lawrence Berkeley National Lab.(LBNL), Berkeley, CA (United States), 1999.

Rutqvist, J.: An overview of TOUGH-based geomechanics models, Computers & Geosciences, 108, 56–63, 2017.

Strebelle, S.: Conditional simulation of complex geological structures using multiple-point statistics, Mathematical geology, 34, 1–21, 2002.

Subramanian, N.: Steel structures-Design and practice, Oxford University Press, 2011.

475 Tarkowski, R.: Underground hydrogen storage: Characteristics and prospects, Renewable and Sustainable Energy Reviews, 105, 86–94, 2019.

Terzaghi, K.: Die Berechnug der Durchlassigkeit des Tones aus dem Verlauf der hydromechanischen Spannungserscheinungen, Sitzungsber. Akad. Wiss.(Wien). Math.-Naturwiss. Kl., Abt. Iia, 132, 125–138, 1923.

Vanmarcke, E., Shinozuka, M., Nakagiri, S., Schueller, G., and Grigoriu, M.: Random fields and stochastic finite elements, Structural safety, 480 3, 143–166, 1986.

Verruijt, A.: Computational geomechanics, vol. 7, Springer Science & Business Media, 1995.

Verruijt, A.: Theory and problems of poroelasticity, Delft University of Technology, 71, 2013.

Verruijt, A.: Numerical and analytical solutions of poroelastic problems, Geotechnical Research, 5, 39–50, 2018.

Wang, H. F.: Theory of linear poroelasticity with applications to geomechanics and hydrogeology, Princeton University Press, 2017.

485 Weng, X.: Modeling of complex hydraulic fractures in naturally fractured formation, Journal of Unconventional Oil and Gas Resources, 9, 114–135, 2015.

Wilkins, A., Green, C. P., and Ennis-King, J.: PorousFlow: a multiphysics simulation code for coupled problems in porous media, Journal of Open Source Software, 5, 2176, 2020.

Xu, L.: Typical values of Young's elastic modulus and Poisson's ratio for pavement materials, 2016.

490 Xu, T., Sonnenthal, E., Spycher, N., and Pruess, K.: TOUGHREACT—a simulation program for non-isothermal multiphase reactive geochemical transport in variably saturated geologic media: applications to geothermal injectivity and CO_2 geological sequestration, Computers & geosciences, 32, 145–165, 2006.

Yang, D., Koukouzas, N., Green, M., and Sheng, Y.: Recent development on underground coal gasification and subsequent CO_2 storage, Journal of the energy institute, 89, 469–484, 2016.

495 Ye, S., Xue, Y., Wu, J., Yan, X., and Yu, J.: Progression and mitigation of land subsidence in China, Hydrogeology Journal, 24, 685–693, 2016.

Zappa, G., Bersezio, R., Felletti, F., and Giudici, M.: Modeling heterogeneity of gravel-sand, braided stream, alluvial aquifers at the facies scale, Journal of Hydrology, 325, 134–153, 2006.

Zaruba, Q. and Mencl, V.: Landslides and their control, Elsevier, 2014.

500 Zhao, H., Jeng, D.-S., Liao, C., and Zhu, J.: Three-dimensional modeling of wave-induced residual seabed response around a mono-pile foundation, Coastal Engineering, 128, 1–21, 2017.